Available online at www.sciencedirect.com
SCIENCE DIRECT®
Journal of Nuclear Materials 326 (2004) 114–124
journal of nuclear materials
www.elsevier.com/locate/jnucmat

Low-temperature low-dose neutron irradiation effects on beryllium

Lance L. Snead *

Metals and Ceramics Division, Oak Ridge National Laboratory, Oak Ridge, TN 37831-6140, USA

Received 28 October 2003; accepted 31 December 2003

Abstract

Mechanical property results are presented for high quality beryllium materials subjected to low-temperature, low-dose neutron irradiation in water-moderated reactors. Materials chosen were the S-65C ITER candidate material produced by Brush Wellman, Kawecki Berylco Industries P0 beryllium, and a high-purity zone refined beryllium. Mini-sheet tensile and thermal diffusivity specimens were irradiated in the temperature range of ~100–300 °C with a fast ($E > 0.1$ MeV) neutron fluence of $0.05–1.0\times10^{25}$ n/m^2 in the high flux isotope reactor (HFIR) at the Oak Ridge National Laboratory and the high flux beam reactor (HFBR) at the Brookhaven National Laboratory. As expected from earlier work on beryllium, both materials underwent significant tensile embrittlement with corresponding reduction in ductility and increased strength. Both thermal diffusivity and volumetric expansion were measured and found to have negligible changes in this temperature and fluence range. Of significance from this work is that while both materials rapidly embrittle at these ITER relevant irradiation conditions, some ductility (1–2%) remains, which contrasts with a body of earlier work including recent work on the Brush-Wellman S-65C material irradiated to slightly higher neutron fluence.

1. Introduction

Beryllium has been considered for nuclear fuel cladding, nuclear fuel compacts and as a neutron moderator for fission power plants dating back to the early 1950s. Other than the non-structural application as a core moderator/reflector, this material has found little use in nuclear applications due to its low ductility even in the absence of irradiation.

The limited ductility of the various types of beryllium is a function of many factors including temperature, chemical purity, grain size and to some extent the rate at which the material is strained. Moreover, the hexagonally close packed beryllium crystal itself is resistant to slip, severely limiting ductility potential of the material. The beryllium hcp crystal has only two operating slip modes (at least at low temperatures) being basal slip $(0\,0\,0\,1)$ and prismatic slip $(1\,\bar{0}\,1\,0)$. For high purity beryllium, ductility can be categorized into three temperature-dependent regimes. In the low temperature regime ($T < 200$ °C) the shear stress required to activate prismatic slip is quite high and failure typically occurs by transgranular fracture of the basal plane. Total elongation in this temperature range for high quality vacuum hot pressed material (e.g. Brush Wellman S-65C at 150 °C) is ~5% in the direction parallel to the pressing direction and ~20% in the transverse direction. As the temperature is increased above this lower temperature regime the critical stress for prismatic slip decreases and both slip modes combine to yield peak total elongations of about 50% both parallel and transverse to the forming direction due to anisotropic texturing of the grains. In this intermediate temperature regime (~200–500 °C) the failure is primarily ductile/fibrous tearing. As the temperature is further increased, intergranular failure begins to occur returning the total elongation to below 20%.

* Tel.: +1-865 574 9942; fax: +1-865 241 3650.
E-mail address: sneadll@ornl.gov (L.L. Snead).

0022-3115/$ - see front matter © 2004 Elsevier B.V. All rights reserved.
doi:10.1016/j.jnucmat.2003.12.016

Irradiation of beryllium with high-energy neutrons has the effect of producing small dislocation loops or 'black spots' at low temperatures (<400 °C) [1–5]. Helium, formed by interaction of beryllium with fast neutrons, forms visible bubbles at temperatures above 325–400 °C [6,7]. The helium bubbles tend to form at grain boundaries from 325 to 600 °C [7–15] and is also reported to decorate dislocations within grains in the temperature range of 450–550 °C [7,8]. In a recent work [16] at high dose (1×10^{26} n/m^2, $E > 0.1$ MeV) at an irradiation temperature of ~100 °C Chakin and Ostrovsky observed a high density of ~20 nm interstitial dislocation loops. No helium bubbles were resolvable until the sample was annealed to greater than 500 °C at which point evenly distributed 1–4 nm bubbles were seen. Because the upper temperature of this study is ~50 °C less than the lowest temperature at which helium bubbles have been observed, the helium is thought to be trapped in submicroscopic clusters at defects or impurity sites within the grain interiors of the beryllium.

Both point defect clusters and helium bubbles adversely affect the mechanical properties of beryllium, regardless of its metallurgical form. Point defect clusters and bubbles impede dislocation motion resulting in a severe reduction in elongation and increased strength [2,3,8,9,11–13,17–22] and hardness [1,8,9,14,18,21]. The irradiation effects database has been reviewed in the past [18,23–25] mainly including work conducted prior to 1970. More recently a number of research groups have been studying the thermomechanical properties of state-of-the-art forms of beryllium for fusion reactor applications [26–33]. Good reviews of the more recent work can be found in the literature [34,35].

The purpose of this work is to present the effects of low-temperature, low-dose neutron irradiation on high-purity beryllium materials with varied levels of beryllium oxide impurity. In particular the as-irradiated mechanical properties and the effect of post-irradiation annealing is studied.

2. Materials, irradiation and experimental techniques

2.1. Materials

Table 1 lists the mechanical properties and impurity levels in the materials chosen for this study. The first material listed is an International Thermonuclear

Table 1
Room temperature properties and chemical impurities of beryllium materials

	Brush Wellman S-65C	Kawecki Berylco P0	Zone refined Be[a]
Yield stress (MPa)			
Longitudinal	257	370	
Transverse	265	405	
Ultimate stress (MPa)			
Longitudinal	381	515	
Transverse	414	460	
Fracture elongation (%)			
Longitudinal	3.5		
Transverse	6.6	4.9	
Density (g/cc)[b]	1.844	1.849	1.846
Impurities			
BeO (wt%)	0.64	3.36	0.01
C (wt%)	0.038	0.173	0.006
Fe (wppm)	670	1000	605
Al	230	120	110
Si	255	70	65
Mg	30	40	5
Zn	<10	NA	10
Ni	<20	95	25
Mn	<20	30	65
Cu	25	15	15
Ti	65	NA	40
Co	8	<5	6
N	120	NA	NA
Cr	50	90	40

[a] Max Planck zone refined Be courtesy of Brush Wellman.
[b] As measured in this study.

Experimental Reactor first wall candidate beryllium, Brush Wellman S-65C. This material is vacuum hot pressed from impact ground Be powder (11–45 μm) at ~1050–1150 °C followed by a 870 °C heat treatment to remove aluminum from solution by forming $AlFeBe_2$ precipitates. The S-65C beryllium was provided by Brush Wellman and designated as process Lot 4880 and is a commercially available, high quality structural beryllium. The grain size of the final product was ~9 μm. The second material chosen for this study was manufactured by the now defunct Kawecki Berylco Industries (KBI) and is designated as P0 (P-zero) taken from billet no. 040. This material was manufactured (≈1975) by vacuum hot pressing impact ground powder (~9 μm) at a temperature of 1065 °C. The grain size of the final product was ~2.9 μm. This was a research grade material processed for reduced impurity content by double electrolytically refining the beryllium powder. The third material studied was Max Planck zone refined beryllium with large grain size (>2 mm) provided courtesy of Brush Wellman. The supplied amount of this material was too limited to allow tensile testing.

From Table 1 significant differences are seen both in vendor supplied mechanical properties and chemical composition for the chosen materials. The strength (at least in the longitudinal direction) is greater for the KBI-P0 material as compared with the S-65C, while the total elongation is somewhat higher for the S-65C. It is interesting to note that, while the KBI-P0 billets of material had very good ductility at the time of their manufacture, the elevated amount of BeO as compared with the BW S-65C (3.36 vs. 0.64 wt%), and possible other metallurgical improvements, yields lower elongation than the present day commercial S-65C beryllium.

Samples were machined by Speedring, Inc. (Cullman, AL) to Brush Wellman specifications. Two sample geometries were fabricated: (1) Type SS-3 mini-sheet tensile specimens (mini-sheet tensile specimens 25.4 mm total length, 8.2 mm in gage length, 0.76 mm in thickness, and 1.52 mm in gage width) and (2) 6 mm diameter, 4 mm thick solid cylinders for thermal diffusivity tests (S-65C only). Mechanical property data in this paper is taken from samples machined in the direction transverse to the forming direction.

2.2. Irradiation exposures

Two water moderated fission reactors were used for the specimen irradiation. The high flux isotope reactor (HFIR) hydraulic tube facility at the Oak Ridge National Laboratory was used to study the effect of fluence at constant irradiation temperature of 300 °C. The SS-3 mini-sheet tensile specimens and thermal diffusivity discs were loaded inside an aluminum holder which was welded inside a 'rabbit' capsule. The capsules were then baked at 200 °C and stored in the presence of hygroscopic media. The rabbit was welded shut in an ultra high purity helium environment. Each rabbit was radiographed and underwent a QA procedure to ensure air or water was unable to penetrate the capsule. Sample temperature was achieved by gas-gap conduction of the nuclear heating between the sample holder and the rabbit body, both made of Type 6061-T6 aluminum. Rabbits were irradiated in the HT-3 position with a thermal and fast ($E > 0.1$ MeV) neutron flux of 7.8×10^{18} and 2.2×10^{19} n/m^2, respectively [36]. Fluences of irradiation were 0.05, 0.2 and 1.0×10^{25} n/m^2 ($E > 0.1$ MeV) at a calculated irradiation temperature of 300 °C.

The high flux beam reactor (HFBR) at the Brookhaven National Laboratory was used to study the effects of varied irradiation temperature (105, 202 and 275 °C) at constant fluence. Capsules were designed for insertion into the V-15 core thimble position. Each capsule consisted of separate gas-gapped subcapsules containing samples. The cover gas was static very high purity helium. Variation in sample temperature in different subcapsules was achieved by varying the gas gap between the subcapsules and the inside of the external capsule, which was in contact with the core coolant water. The subcapsule bodies were electro-discharge machined from Type 6061-T6 aluminum. Each subcapsule typically contained four SS-3 tensile specimens. After the samples were loaded, a Type 304 stainless steel roll pin (a spring) was used to ensure that the specimens were in good thermal contact with the subcapsule holder. A type-K thermocouple was embedded in each holder monitoring temperature throughout the HFBR irradiation. During irradiation, sample temperatures were recorded continuously. The temperature variation for two HFBR irradiations were always less than 12 °C.

At the time of these irradiations the HFBR was operating at 30 MW_{th} power. Greenwood and Ratner [37] has conducted a calculation on a single dosimetry sample near the center of the V-15 thimble and these dosimetry results were assumed for this report. Each of the HFBR capsules was irradiated for an estimated thermal and fast ($E > 0.1$ MeV) fluence of $\sim2.3\times10^{24}$ and $5.5\pm0.2\times10^{24}$ n/m^2, respectively. For the remainder of the paper quoted fluence numbers are given as $E > 0.1$ MeV fluences unless otherwise specified.

Based on calculations made by Gabriel et al. [38] and using the revised spectra of the HFBR provided by Greenwood and Ratner [37] the helium concentration and displacements per atom (dpa) for the various irradiations are listed in Table 2. For these calculations a displacement energy (E_d) of 25 eV was assumed. Note that due to the relatively higher flux at high neutron energies, the HFBR V-15 spectrum produced a slightly higher He/dpa ratio than the HFIR hydraulic tube position.

Table 2
Irradiation conditions

	Thermal fluence, $\times 10^{25}$ n/m^2	Fast fluence, $\times 10^{25}$ n/m^2 ($E > 0.1$ MeV)[a]	Fast fluence, $\times 10^{25}$ n/m^2 ($E > 1.0$ MeV)	dpa	He conc. (appm)	He/dpa
HFIR (300 °C)	0.14	0.05	0.026	0.04	10	
	0.6	0.20	0.11	0.16	42	254
	2.8	1.0	0.53	0.82	208	
HFBR (95–278 °C)	0.23	0.5 ± 0.02	0.21 ± 0.02	0.34	250	824

[a] Energy cut-off is listed as $E > 0.11$ MeV for HFBR results [37].

2.3. Experimental techniques

Thermal diffusivity was measured at room temperature (~22 °C) using a custom built thermal flash (xenon laser) apparatus. Following the thermal flash on the front surface, the rear surface temperature was measured by the infrared signal and the diffusivity calculated following Clark and Taylor's analysis [39]. For the thermal diffusivity calculations the density was calculated by dry weight and physical dimensions. The thermal diffusivity and dimensions of every specimen were measured before and after irradiation.

The room temperature thermal conductivity (K) was calculated using the measured thermal diffusivity (α), measured density (ρ), and the specific heat (C_p) as follows:

$$K = \alpha \rho C_p. \quad (1)$$

The conversion from thermal diffusivity to thermal conductivity used the assumption that the specific heat remained unchanged with irradiation. The repeatability of density measurement was seen to be better than 1%, which is assumed as the relative accuracy.

Density was determined for calculation of swelling by using a density gradient column according to ASTM D1505-89 utilizing chemical mixtures of trichloroethane and ethylene bromide and calibrated glass floats [40]. The linear density gradient of the column was 0.35 (mg/cm^3)/cm yielding an accuracy of relative density change of approximately 0.005%. Prior to dropping the samples in the density gradient column all specimens were etched in a mixture of hydrofluoric acid and ethyl alcohol and then dried. Visible etching and etch pits were observed.

Tensile testing was performed in load control digitally recording the cross-head displacement and applied load. Elevated temperature testing was performed in static argon with the thermocouple in contact with a sample grip. Room temperature testing was in air. The specimens were held at the test temperature for at least 15 min prior to applying tensile load. In both non-irradiated and irradiated conditions the S-65C specimens were pin-loaded while the irradiated P0 specimens had to be shoulder loaded due to their tendency for failure at the pin-holes. A cross-head displacement rate that produced an initial strain rate of 0.001/s was applied for the SS-3 mini-sheet tensile specimens. This strain rate is approximately the same as that used in the recent European ITER beryllium irradiation program [29,30,28] although it is about an order of magnitude higher than the value recommended by the Materials Advisory Board [41]. The effect of increasing strain rate in beryllium is to reduce the temperature at which beryllium moves from brittle to ductile failure. However, this temperature shift is expected to be small for the strain rate differences noted here [42,43], though the general effect of strain rate on failure warrants further study, especially for irradiated material.

A Buehler Micromet 3 microhardness testing machine was used at 500 g and 1 kg loads to measure the Vickers hardness. The two loads gave essentially the same hardness values and 500 g loading is reported here. Specimens were prepared for hardness testing by lapping with diamond film in oil. Potential effects of the surface polish on the hardness were dismissed by observing no difference between unprepared and prepared surfaces of non-irradiated material over a wide range of loading.

3. Results

3.1. Swelling and thermal conductivity

The effect of irradiation at the doses and temperatures studied had essentially no effect on the thermal conductivity or density of the materials selected. The density of the S-65C beryllium was measured to be 1.844 g/cc, or 99.82% of pure beryllium theoretical density (%$_{td}$) while the density of the P0 beryllium was 1.849%$_{td}$ or 100.05 %$_{td}$. The higher than theoretical density of the P0 material can be explained by the elevated level of BeO (3.36 wt% at ~3.0 g/cc density) in this material, as seen in Table 1. Upon irradiation, swelling occurred in all materials, though the amount of swelling was very small. The largest swelling occurred for the HFIR material irradiated to 1×10^{25} n/m^2 at approximately 300 °C yielding $+0.027 \pm 0.005$% for the S-65C material and

$0.038 \pm 0.005\%$ for the P0 material. The swelling of the HFBR materials was less than this (~0.02%) and no difference with respect to the irradiation temperature was observed.

The room temperature thermal conductivity of non-irradiated S-65C beryllium was measured to be 184 ± 5 W/m K. This was found using the measured thermal diffusivity and non-irradiated density and specific heat (1.768 J/g K) extrapolated from published S-65C data [44]. It is noted that the calculated thermal conductivity is somewhat lower (about 8%) than that published by Smith [44]. For the case of the material irradiated to 1×10^{25} n/m^2 ($E > 0.1$ MeV) at ~300 °C, the thermal conductivity was within the 4% experimental error of the non-irradiated value.

3.2. Hardness

The irradiation induced hardening of these beryllium materials as a function of dose and temperature is given in Figs. 1 and 2, respectively. The elevated level of BeO in the KBI-P0 material contributed to the higher initial hardness for this material as compared to the S-65C. Specifically, the room temperature non-irradiated Vicker's hardness was measured to be 228 ± 3 kg/mm^2 as compared to 181 ± 2 kg/mm^2 for S-65C. A modest increase hardness was observed at 300 °C for a HFIR fluence of 0.05×10^{25} n/m^2 for the P0 material while a larger increase was seen for both materials following 0.2×10^{25} n/m^2. As fluence was further increased to 1.0×10^{25} n/m^2 the hardness of both materials substantially increased. As seen in Fig. 2, the dependence of hardness on HFBR irradiation temperature is significantly different for the two materials. The P0 material

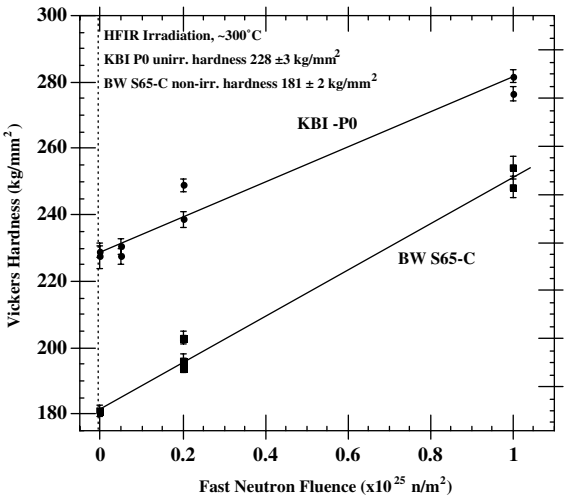

Fig. 1. The effect of HFIR neutron irradiation fluence at 300 °C on room temperature hardness.

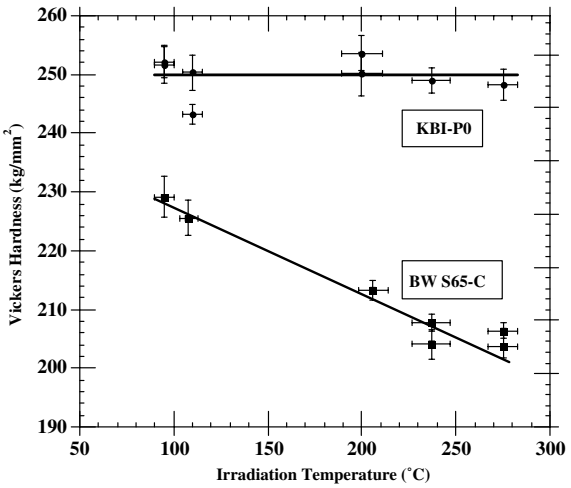

Fig. 2. The effect of HFBR irradiation temperature at a fluence of 0.5×10^{25} n/m^2 on hardness.

appears to have a weak dependence on irradiation temperature while the irradiation hardening (ΔH) for the S-65C is significantly lower for irradiation temperatures >205 °C compared to the 110 °C irradiation value.

The zone-refined beryllium was irradiated in HFBR at one irradiation temperature and dose (95 ± 5 °C and $5 \pm 0.5 \times 10^{24}$ n/m^2, $E > 0.1$ MeV). In comparing the change in hardness for each material at this irradiation condition, the KBI-P0 hardened by ~23 kg/mm^2, the S-65C by ~40, and the highly pure zone refined beryllium by 60 (increasing from ~110 to 180 kg/mm^2).

The effect of isochronal annealing (1 h in argon) on irradiation-induced hardness and density is shown in Fig. 3 for specimens irradiated in HFBR at 95 °C. Noting that the temperature increments were somewhat large (100 °C), it appears that the three materials begin to undergo expansion at anneal temperatures greater than 800 °C. Above 1000 °C the S-65C and zone refined materials swell more dramatically as compared to the P0 beryllium. The hardness change curves in Fig. 3 clearly show a reduction in the irradiation-induced hardening for annealing temperature above 600 °C. Similar to density, the annealing stage above 1000 °C yields a more precipitous drop in hardness for S-65C and zone refined beryllium as compared to the P0.

3.3. Tensile properties

The effects of the neutron irradiation on the tensile properties of both types of beryllium are given in Figs. 4–9. These figures plot the tensile data as a function of irradiation temperature for a constant HFBR dose and as a function of HFIR dose at a constant irradiation temperature. The elongation specified is the total (fracture) elongation while the yield strength is defined at the

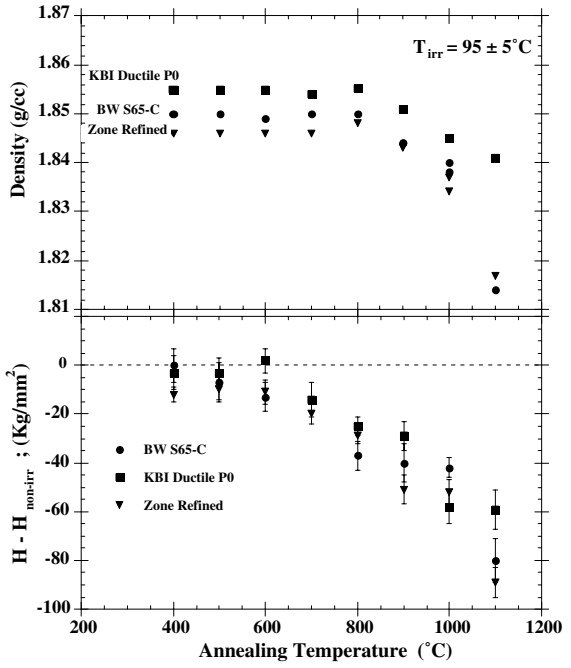

Fig. 3. The effect of HFBR isochronal annealing on hardness and density of Be specimens irradiated in HFBR at 95 °C to 0.5×10^{25} n/m^2.

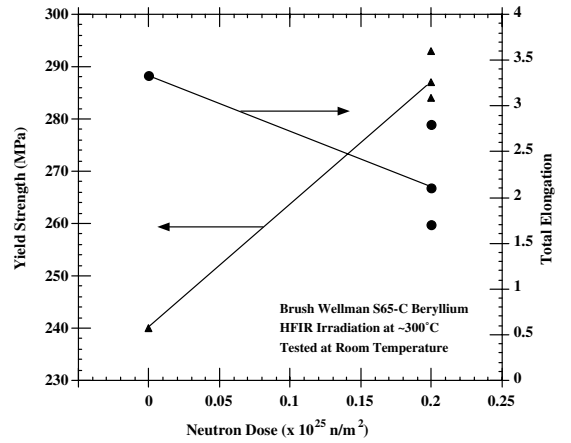

Fig. 4. The effect of HFIR neutron irradiation on strength of S-65C at ambient temperature.

0.2% offset yield. Specific dpa and helium concentration limits are found in Table 2.

As seen in Figs. 4 and 5, the effect of the HFIR neutron irradiation at 300 °C on the S-65C material to a fluence of 0.2×10^{25} n/m^2 is to slightly increase the yield and ultimate tensile strength and reduce the total

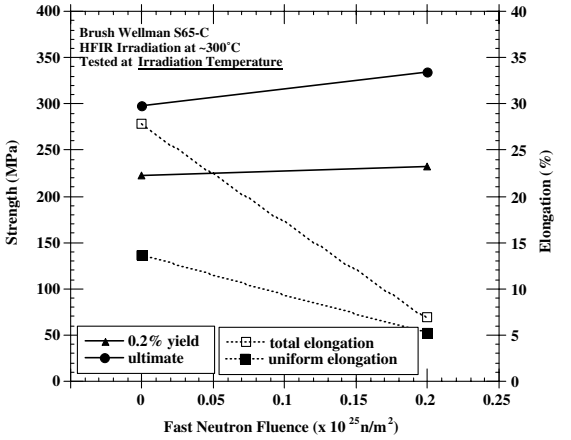

Fig. 5. The effect of HFIR neutron irradiation on strength of S-65C at the irradiation temperature.

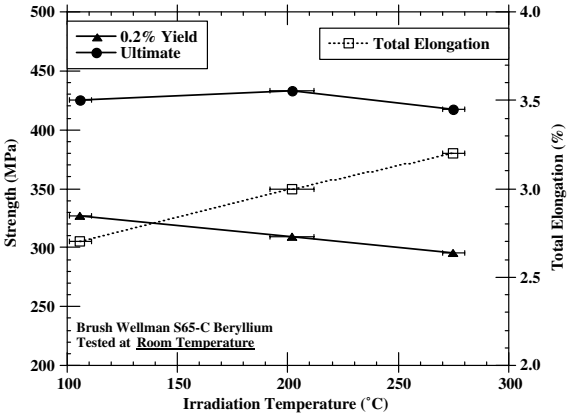

Fig. 6. The effect of HFBR irradiation temperature on the strength of S-65C at ambient test temperature.

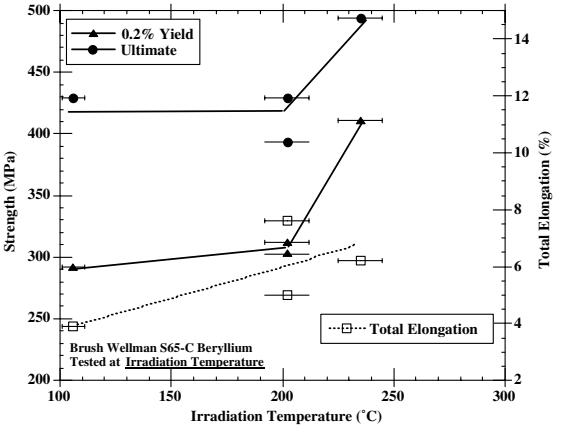

Fig. 7. The effect of HFBR irradiation temperature on the strength of S-65C at the irradiation temperature.

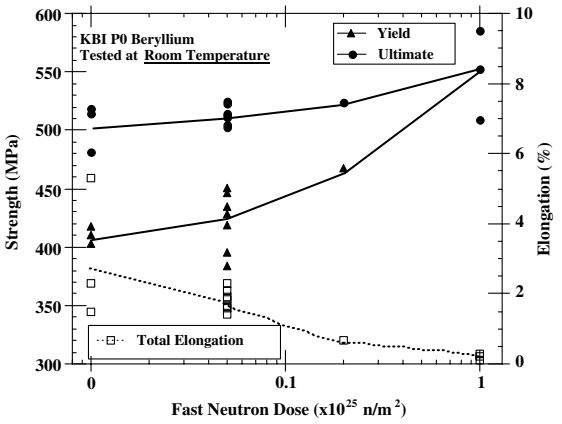

Fig. 8. The effect of HFIR neutron dose on strength of KBI P0 beryllium tested at room temperature.

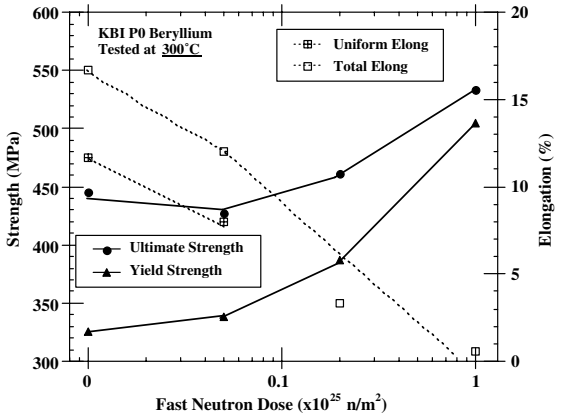

Fig. 9. The effect of HFIR neutron dose on strength of KBI P0 beryllium tested at the irradiation temperature.

elongation. In the irradiated condition both room temperature and 300 °C tensile curves exhibited ductile failure with ~2% and ~5% total elongation at failure (compliance corrected), respectively.

For the irradiation temperature range shown in Fig. 6, the yield strength at room temperature decreases with increasing irradiation temperature, while the total elongation increases slightly. Failure occurs before the onset of necking. The room temperature UTS is nearly independent of irradiation temperature. Fig. 7 shows the same irradiation conditions as plotted in Fig. 6, though for testing conducted at the irradiation temperatures. The trend toward increasing total elongation with increased temperature is still apparent. At the 235 °C irradiation temperature a significant increase in both yield and ultimate strength is observed. It is noted that the data points in Figs. 4–9 represent single sample tests and as seen from the 202 °C irradiation of Fig. 7 (and in Figs. 4 and 8), there is a fair scatter in the tensile data (in contrast with the hardness data (Figs. 1 and 2)). It is clear from the significant increase in hardness at 300 °C from the 0.2 to 1.0×10^{25} n/m^2 level, as well as recent tensile and fracture toughness data on S-65C material irradiated to higher doses [29], that the S-65C material will continue to harden as dose is increased and will eventually become completely embrittled.

Figs. 8 and 9 gives the dose-dependent tensile properties at room temperature and at the irradiation temperature, respectively, for the KBI P0 material irradiated in the HFIR at 300 °C.

4. Discussion

The very low swelling levels in this work are consistent with the work of Gol'tsev et al. [45] predicting a swelling $\Delta V/V = 8.2\times10^{-25}\Phi t$, where Φt is the fast fluence in n/cm^2 ($E > 0.85$ MeV) making the assumption that irradiation temperature is low enough to preclude significant helium diffusion and bubble nucleation and growth. Applying this formulation yields 0.05% for the higher-dose materials of this study compared with the measured values of 0.027 to 0.038 ± 0.005% for S-65C and P0, respectively. Further, the model developed by Dalle-Donne et al. [46] predicts near-zero swelling in the temperature and fluence range of this study. It is noted that the temperatures at which the materials were irradiated here were below the lowest temperature at which resolvable helium bubbles have been observed [2,23] and is therefore in a region where point defect and submicroscopic helium cavity strain is responsible for swelling. A significant reduction in thermal conductivity is not expected unless the material is irradiated in the temperature, fluence or solute range where helium bubble formation and swelling becomes pronounced (about >350 °C).

The previous work on annealing of hardening centers in powder-metallurgy processed beryllium irradiated at 'pile temperatures' of less than 100 °C inferred that the embrittlement [47] and recovery kinetics [14,21,48] were dependent on irradiation temperature and dose, with no specific mention of metallurgical form. In this early work the hardening was attributed, at least for temperatures of <200 °C, to solid solution hardening effects caused by the helium, with additional helium hardening at the grain boundaries. The source of hardening in beryllium, whether due to helium clusters (Orowan hardening) or through point defect induced solid solution strengthening was recently addressed in work by Kesternich and Ullmaier [49] which concluded that the point defect strengthening was insignificant, while the Orowan hardening yielded the correct order of magnitude hardening. This work was based on results obtained using helium implantation [49] and by comparison to the

neutron irradiation results presented in this paper and published by Moons [49].

For the three materials of this study, it was observed that the absolute hardening (ΔH) for the ~95 °C irradiations was significant, with slightly greater hardening for the lower BeO content, lower initial hardness materials. Noting that the zone refined beryllium, which is essentially single crystal from the standpoint of indentation testing, hardened in a consistent manner with the other materials it can be reasonably concluded that hardening is caused by a combination of submicroscopic helium clusters along with irradiation-produced defect clusters. At least for low temperature irradiation the grain boundaries do not play a significant role in hardening.

The relative insensitivity of hardness on irradiation temperature for the P0 material (Fig. 2) in comparison to the lower BeO content S-65C suggests that the BeO may serve to trap the helium. As the BeO is responsible for the higher initial hardness of this material, and is thermally stable, the material appears insensitive to irradiation temperature (over this narrow low-temperature range). This is reinforced by noting that the P0 material is more resistant to annealing effects on hardness and density (Fig. 3) at the temperatures at which large helium bubbles are forming.

Hickman and Stevens [48] as well as Weir [14] found hardening in low-temperature irradiated beryllium upon annealing in the 400–500 °C range followed by a gradual recovery to non-irradiated hardness levels by ~800 °C for material irradiated to $<6\times10^{24}$ n/m^2 (nvt), ~58 appm He. Rich et al. [50] observed similar behavior in materials irradiated to $\sim7.6\times10^{25}$ n/m^2 ($E>1$ MeV), ~2000 appm He, though the material continued to soften well below the non-irradiated hardness. These researchers all attributed the annealing effects to the coalescence of trapped helium into larger bubbles. This was supported by evidence of swelling and TEM observation. The data in Fig. 3 shows the effect of isochronal annealing of the high-purity materials of this study. Results are similar to that seen in the earlier works. Specifically, the swelling at high temperature as well as the reduction in hardness occur at about the same annealing temperatures, though it can be reasonable argued that a recovery in hardness occurs at ~200 °C lower than the density change. Unfortunately, the data are insufficient to discriminate between the possible recovery mechanisms, i.e. loop annihilation and helium bubble growth. All materials of this studied yielded lower hardness after annealing above 600 °C, as compared with their non-irradiated values. This result was observed by both Stevens [48] and Rich [50]. However, from the lower data-set in Fig. 3 it is clear that the hardening behavior observed by both Hickman and Stevens [48] as well as Weir [14] at intermediate annealing temperatures (~400–700 °C) was not observed in the present study. Given that the temperatures and doses of the previous and current work were similar it is speculated that the source of the error was statistical in nature. While purity of material was not given by Hickman and Stevens, it is noted that the Weir material had about 2.4 wt% BeO, which is near that of the P0 material of this study, but significantly higher than the S-65C. Also, the metallic impurity content for the Weir material was a factor of a few to ten times the levels given in Table 1.

In the comprehensive work by Moons et al. [30] and Chaouadi et al. [29] on vacuum hot pressed S-65B, which has very similar BeO content (0.63 wt%) and processing to the S-65C of this study, materials were irradiated over similar fluence and temperature range to the data presented here. While their work applied a slightly slower strain rate (5.5×10^{-4}/s up to 1% elongation and 1.25×10^{-5}/s beyond) compared to our 0.001/s and utilized circular cross section samples compared to our rectangular cross section samples, the basic irradiation-induced trends were similar. Specifically, for the comparable temperature and dose ranges, significant

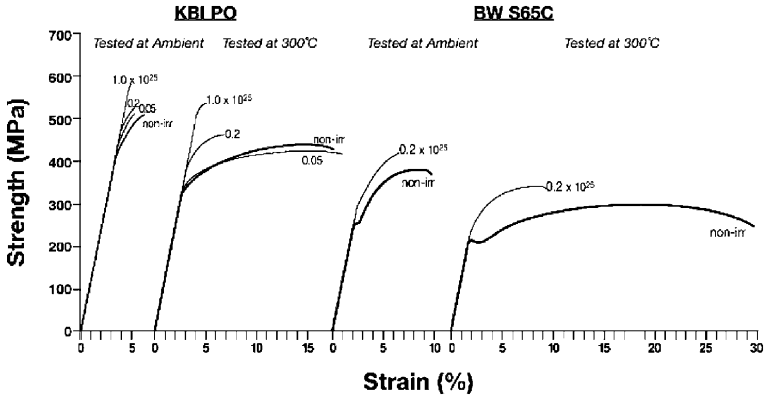

Fig. 10. Load vs. elongation curves of specimens irradiated in HFIR at 300 °C.

hardening and embrittlement occurred by $\sim 1 \times 10^{25}$ n/m^2. One difference between the present work and other work on modern, high-purity beryllium [26–33] is that a small degree of ductility is seen here in the S-65C material at a fluence and temperature where the previous work notes complete embrittlement. This observation is illustrated by inspection of the engineering tensile curves for both KBI P0 and S-65C HFIR irradiated at 300 °C are given in Fig. 10. The non-irradiated KBI material shows very limited ductility and exhibits no reduction in area near room temperature. Upon irradiation the engineering strength increases and the total elongation is reduced until the P0 material becomes very brittle by a fluence of 1×10^{25} n/m^2 for testing both at ambient and at the irradiation temperature. This general trend in tensile hardening is in agreement with the Vicker's hardness data given in Fig. 1. By contrast, the S-65C material shows 6.5% total elongation at room temperature which is reduced to ~2% at the 0.2×10^{25} n/m^2 dose level. For the same dose conditions the total elongation for testing at the irradiation temperature is reduced from 27.8% to 6.9%, each showing signs of necking after the ultimate strength is reached (Fig. 10).

The mode of fracture for the 0.2×10^{25} n/m^2 HFIR irradiated S-65C beryllium was determined using SEM fractography, with selected images given in Fig. 11. Fig. 11(A) and (B) show images of the fracture surface and selected areas on the fracture surface of non-irradiated S-65C tested at ambient temperature and 300 °C, respectively. It is noted that significant uniform elongation and reduction in area (~30%) was observed in the 300 °C testing case (Fig. 11(B)). The mode of fracture was predominantly ductile tearing, though a very limited amount of intergranular failure was observed. For testing at ambient (Fig. 11(A)) no significant reduction in area was observed with failure comprised predominantly of ductile tearing. Limited intergranular failure and transgranular cleavage was observed. No significant reduction in area (<5%) was seen in any irradiated beryllium in this study. Fig. 11(C) and (D) gives the fracture surfaces for S-65C beryllium irradiated to 0.16 dpa at ~300 °C. For the case of testing at the irradiation temperature (Fig. 11(D)) the fracture mode was a mix of ductile tearing with a significant intergranular failure. Testing of similar samples at ambient temperature (Fig. 11(C)) intergranular failure became more dominant with significant areas of transgranular cleavage present (Fig. 11(D)).

Similar 'limited ductility' was also seen for the higher dose, lower temperature HFBR irradiated samples. Total elongations of ~3% (cf. Fig. 6) for the 0.55×10^{25} n/m^2 HFBR irradiated specimens were observed for room temperature testing. As seen from Figs. 7 and 10, S-65C samples tested at the irradiation temperature exhibited total elongation of 5–7%, which contrasts to the very low (<1%) values of the KBI P0 material and

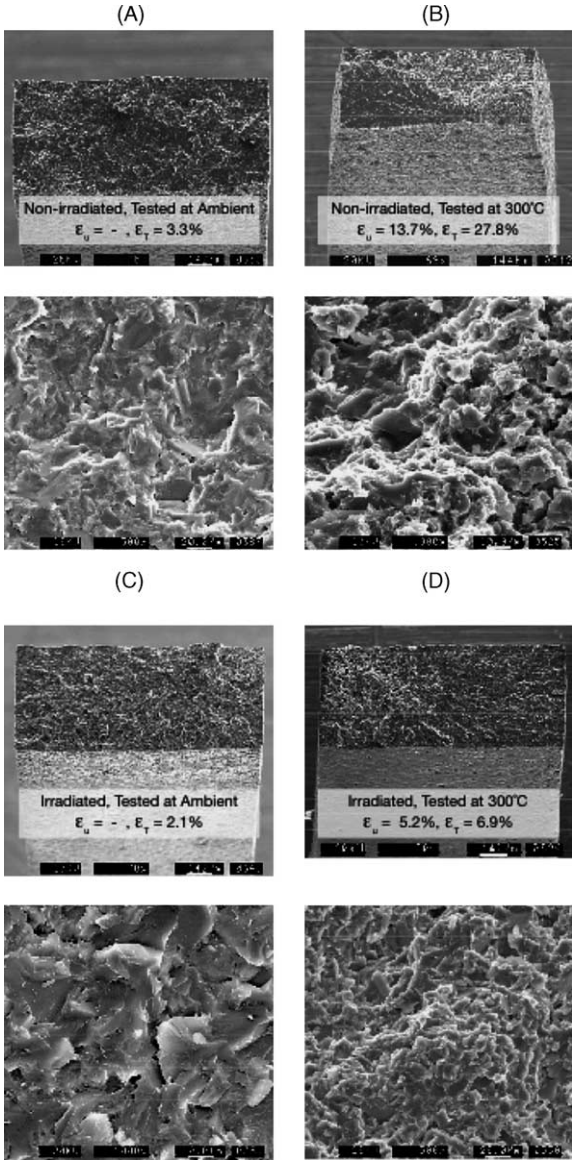

Fig. 11. Fracture surfaces of non-irradiated and 0.2×10^{25} n/m^2 HFIR irradiated S-65C specimens.

similarly irradiated beryllium forms in the literature, including the S-65B material studied by Moons et al. [30] and Chaouadi et al. [29]. As direct comparison, Chaouadi et al. [29] quotes S-65 beryllium irradiated at temperatures of 185–310 °C to $0.65–0.85 \times 10^{25}$ n/m^2 ($E > 0.1$ MeV) range (similar to the fluence of this study). Results for this material, both for testing at ambient and irradiation temperature, gave uniform and total elongations of less than 0.1%. Shown in Fig. 12 are the tensile curves for samples of S-65C, HFBR irradiated at 205 °C to 0.55×10^{25} n/m^2 ($E > 0.1$ MeV). When the samples were tested at the irradiation temperature,

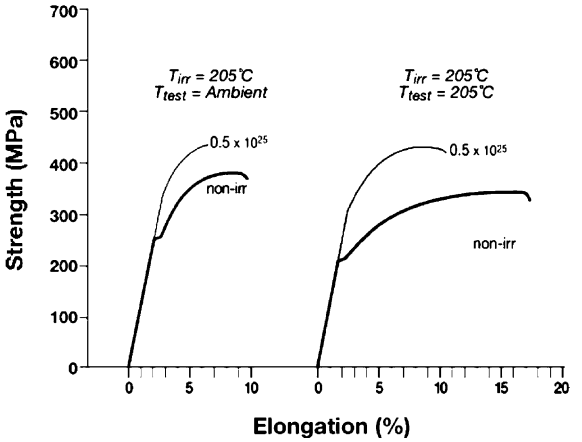

Fig. 12. Tensile load vs. elongation curves of specimens irradiated in HFBR at 205 °C to a fluence of 0.55×10^{25} n/m^2.

total (and uniform) elongation was reduced from 14.6% (6.7%) to 6.9% (5.2%) following irradiation. When tested at ambient temperature, plastic instability was only seen in the non-irradiated sample with total elongation reduced from ~6.5% to ~3%.

5. Conclusions

This paper has presented results of irradiated thermophysical properties of select, high-quality beryllium. The overall results on swelling, thermal conductivity, and tensile properties are in good agreement with present work on similar materials and qualitative with the older literature data on less pure beryllium forms. Comparison of hardening and annealing behavior for the zone refined and powder processed materials indicate that hardening is not dominated by helium stabilized defects forming along grain boundaries. For the two materials that underwent tensile testing, the lower BeO content Brush Wellman S-65C material showed less severe embrittlement, retaining a small, but meaningful level of ductility following irradiation. This result is in contrast to other recent work on S-65B, which found that similar irradiation condition yielded extremely low or complete embrittlement.

Acknowledgements

The author would like to thank Dave Dombrowski and the Brush Wellman company for provision of the S-65C material as well as for valuable technical assistance. I would also like to thank Ben Odegard of the Sandia National Laboratory for providing the materials and pertinent information regarding the Kawecki Berylco Industries P0 material. Technical help was also provided by J.P. Strizak, J.L. Bailey, and A.M. Williams for which I am grateful. Research sponsored by the Office of Fusion Energy Sciences, US Department of Energy under contract DE-AC05-00OR22725 with UT-Battelle, LLC.

References

[1] J.B. Rich, G.P. Walters, in: The Metallurgy of Beryllium, Institute for Metals Monograph No. 28, Chapman and Hall, London, 1961, p. 362.
[2] J.M. Beeston et al., in: Proceedings of the Symposium on Materials Performance in Operating Nuclear Systems, CONF-730801, 1973, p. 59.
[3] G.P. Walters, J. Less, Common Metals 11 (1966) 77.
[4] D.S. Gelles, H.L. Heinisch, J. Nucl. Mater. 191–194 (1992) 194.
[5] R.S. Barnes, in: The Metallurgy of Beryllium, Institute of Metals Monograph and Report Series No. 28, Chapman and Hall, London, 1961, p. 372.
[6] J.M. Beeston, L.G. Miller, E.L. Wood Jr., R.W. Moir, J. Nucl. Mater. 122&123 (1984) 802.
[7] D.S. Gelles, G.A. Sernyaev, M.D. Donne, H. Kawamura, J. Nucl. Mater. 212–215 (1994) 29.
[8] J.B. Rich, G.P. Walters, Metall. Beryllium 4 (1961) 362.
[9] B.S. Hickman, G. Bannister, Report Part 2, AAEC/E-115 (also TRG Report 540 UKAEA), 1963.
[10] B.S. Hickman et al., Report UKAEA TRG Report 540, 1963.
[11] G.T. Stevens, B.S. Hickman, Report AAEC/E-133, 1965.
[12] J.M. Beeston, in: Effects of Radiation on Structural Materials, ASTM-STP, vol. 426, ASTM, Philadelphia, PA, 1967, p. 135.
[13] E.D. Hyam, G. Sumner, in: Radiation Damage in Solids, vol. 1, IAEA, Vienna, 1962.
[14] J.R. Weir, in: The Metallurgy of Beryllium, Institute of Metals Monograph and Report Series No. 28, Chapman and Hall, London, 1961, p. 395.
[15] R. Sumerling, E.D. Hyam, in: The Metallurgy of Beryllium, Institute of Metals Monograph and Report Series No. 28, Chapman and Hall, London, 1961, p. 381.
[16] V.P. Chakin, Z.Y. Ostrovsky, J. Nucl. Mater. 307–311 (2002) 657.
[17] E.H. Smith et al., in: Proceedings of the Symposium on the Physical Metallurgy of Beryllium, Gatlinburg, CONF-730801, 1973, p. 41.
[18] J.M. Beeston, Nucl. Eng. Des. 14 (1970) 445.
[19] J.M. Beeston, G.R. Longhurst, R.S. Wallace, A.P. Abeln, J. Nucl. Mater. 195 (1992) 102.
[20] M.H. Bartz, in: Properties of Reactor Materials, vol. 5, Second United Nations Conf. on the Peaceful Uses of Atomic Energy, United Nations, Geneva, 1958, p. 466.
[21] B.S. Hickman, in: The Metallurgy of Beryllium, Institute of Metals Monograph and Report Series No. 28, Chapman and Hall, London, 1961, p. 410.
[22] S. Morozumi, S. Goto, M. Kinno, J. Nucl. Mater. (1977) 82.
[23] D.S. Gelles, J.F. Stubbins, J. Nucl. Mater. 212–215 (1994) 778.
[24] F. Scaffidi-Argentina, G.R. Longhurst, V. Shestakov, H. Kawamura, J. Nucl. Mater. 283–287 (2000) 43.

[25] M. Dalle-Donne, G.R. Longhurst, H. Kawamura, F. Scaffidi-Argentina, J. Nucl. Mater. 258–263 (1998).
[26] A.S. Pokrovsky, S.A. Fabritsiev, R.M. Bagautdinov, Y.D. Goncharenko, J. Nucl. Mater. 233–237 (1996) 841.
[27] I.B. Kupriyanov, V.A. Gorokhov, G.N. Nikolaev, V.N. Burmistrov, J. Nucl. Mater. 233–237 (1996) 886.
[28] F. Moons, R. Chaouadi, J.L. Puzzolante, Fusion Eng. Des. 41 (1998) 187.
[29] R. Chaouadi, F. Moons, J.L. Puzzolante, SCK.CEN, Mol, Belgium Report TEC97/51/F040010/15/RC, 1997.
[30] F. Moons, L. Sannen, A. Rahn, J. VanDeVelde, J. Nucl. Mater. 233–237 (1996) 823.
[31] G.A. Sernyaev, A.V. Kozlov, V.R. Barabash, J. Nucl. Mater. 271&272 (1999) 123.
[32] E. Ishitsuka, H. Kawamura, Fusion Eng. Des. 41 (1998) 195.
[33] V.P. Chakin et al., J. Nucl. Mater. 307–311 (2002) 647.
[34] V. Barabash et al., J. Nucl. Mater. 283–287 (2000) 138.
[35] A. Khumutov et al., J. Nucl. Mater. 307–311 (2002) 630.
[36] S.T. Mahmood, S. Mirzadeh, K. Farrell, J.F. Pace, Oak Ridge National Laboratory, Oak Ridge Report ORNL/TM–12831, 1995.
[37] L.R. Greenwood, R.T. Ratner, in: Fusion Materials Semiannual Progress Report for Period Ending, 31 December 1997, vol. DOE/ER-0313/23, 1998, p. 309.
[38] T.A. Gabriel, B.L. Bishop, F.W. Wiffen, Oak Ridge National Laboratory, Oak Ridge Report ORNL/TM-6361, 1979.
[39] L.M. Clark, R.E. Taylor, J. Appl. Phys. 46 (1975) 114.
[40] ASTM, D1505-85, Standard Test Method for Density of Plastics by Density Gradient Technique, 1985.
[41] X, Tests Methods Subcommittee Committee on Beryllium Metallurgy. National Academy of Sciences, National Research Council, Washington Report Publication MAB-205-M.
[42] A.J. Martin, G.C. Ellis, in: The Metallurgy of Beryllium, Institute of Metals Monograph and Report Series No. 28, Chapman and Hall, London, 1961, p. 3.
[43] G.L. Turner, in: D. Webster, G.J. London (Eds.), Beryllium Science and Technology, vol. 1, Plenum, 1979, p. 145.
[44] M.F. Smith, Fusion Technol. 8 (1985) 1174.
[45] V.P. Gol'tsev, G.A. Sernyaev, Z.I. Chechetkina, Nauka i Teknika, Minsk, 1977.
[46] M. Dalle-Donne, F. Scaffidi-Argentina, C. Ferrero, C. Ronchi, J. Nucl. Mater. 212–215 (1994) 954.
[47] B.S. Hickman, in: G.J. Dienes (Ed.), Studies in Radiation Effects, Series A, Physical and Chemical, vol. 1, Gordon and Breach, 1966, p. 72.
[48] B.S. Hickman, G.T. Stevens, Report Australian Atomic Energy Commission, Report AAEC/E109, 1961.
[49] W. Kesternich, H. Ullmaier, J. Nucl. Mater. 312 (2003) 212.
[50] J.B. Rich, G.B. Redding, R.S. Barnes, J. Nucl. Mater. 1 (1959) 96.